Plant water use responses along secondary forest succession during the 2015-2016 El Niño drought in Panama

Mario Bretfeld, Brent E Ewers, Jefferson S Hall

March 2018

New Phytologist

DOI10.1111/nph.15071

Summary

- Tropical forests are increasingly subjected to hotter, dryer conditions due to global climate change. The effects of drought on forests along successional gradients remain poorly understood.
- We took advantage of the 2015/16 El Niño event to test for differences in drought response along a successional gradient by measuring sap flow in 76 trees, representing 42 different species, in 8, 25, and 80-year old secondary forests in the 15 km^2 "Agua Salud Project" study area, located in central Panama.
- Average sap velocities and sapwood-specific hydraulic conductivities were highest in the youngest forest. During the dry-season drought, sap velocities increased significantly in the 80-year old forest due to higher evaporative demand but not in younger forests. Main drivers of transpiration shifted from radiation to vapor pressure deficit with progressing forest succession. Soil volumetric water content was a limiting factor only in the youngest forest during the dry season, likely due to less root exploration in the soil.
- Trees in early-successional forests displayed stronger signs of regulatory responses to the 2015/16 El Niño drought, and the limiting physiological processes for transpiration shift from operating at the plant-soil interface to the plant-atmosphere interface with progressing forest succession.

Keywords

Agua Salud, drought, El Niño, plant hydraulics, sap flow, seasonal tropics, secondary forest, succession

Introduction

Ecosystems worldwide are subjected to increasing pressure from climate change and plant water use traits are a crucial component towards developing a predictive understanding of plant responses to these changes. Globally, 2015 marked the warmest year since the beginning of instrumental data collection with temperature anomalies exceeding two standard deviations in the tropics (Hansen & Sato, 2016). Tropical forests are particularly sensitive to drought and respond with considerable changes in species distribution and composition (Engelbrecht *et al.*, 2007; Nepstad *et al.*, 2007; Phillips *et al.*, 2009; Wright, 2010). The 2015/16 El Niño-Southern Oscillation (ENSO) event provided an excellent research opportunity to study the responses of tropical forests to severe drought conditions. In Panama, the 2015/16 ENSO event resulted in the third longest dry season on record (173 days) with over 90% of the country experiencing severe drought conditions. A mechanistic understanding of responses to drought of tropical forests is critical to land management and conservation efforts, and to improve the predictive power of global models of carbon and water fluxes that generally perform poorly under drought conditions (Powell *et al.*, 2013).

Hydraulic failure is a main driver of drought-induced tree mortality in tropical forests (Rowland *et al.*, 2015). However, studies that assess drought responses of tropical trees across a successional gradient are often based on seedlings/saplings or monospecific stands (e.g. Huc *et al.*, 1994; Tyree *et al.*, 2003; Engelbrecht *et al.*, 2006; Markesteijn *et al.*, 2011; Pineda-Garcia *et al.*, 2012; Pineda-García *et al.*, 2015), and field data are sparse. Due to the high taxonomic diversity and lack of species dominance in most tropical forests, a trait-based approach to data analysis (McGill *et al.*, 2006; Escudero & Valladares, 2016) is often the only cost-effective way to study these forests. For example, leaf and stem hydraulic traits explained drought tolerance across species in Amazon rainforest trees (Powell *et al.*, 2017), and similar morphological characteristics (e.g. sapwood depth, tree size, phenology) appear to outweigh taxonomic affiliation, as indicated by considerable convergence in sap flow among phylogenetically diverse but morphologically similar species in tropical systems (Meinzer *et al.*, 2001; O'Brien *et al.*, 2004; McJannet *et al.*, 2007; Kunert *et al.*, 2010; Moore *et al.*, 2017). Recent work on sap flow in subtropical and tropical biomes includes assessments of responses to drought (Luo *et al.*, 2016), environmental factors (Eller *et al.*, 2015; Aparecido *et al.*, 2016), and seasonal variability (Kunert *et al.*, 2010; Schwendenmann *et al.*, 2015).

Early-successional, light-demanding species are generally characterized by lower wood density, larger vessel diameter and specific leaf area, coinciding with and higher hydraulic conductivity and sap velocities compared to late-successional species (Bazzaz & Pickett, 1980; Poorter *et al.*, 2004; Poorter *et al.*, 2010; Markesteijn *et al.*, 2011; Apgaua *et al.*, 2015; Schönbeck *et al.*, 2015). Although these traits suggest that early-successional species are more vulnerable to xylem cavitation (Tyree & Sperry, 1989),

some studies report no difference (Pineda-Garcia *et al.*, 2012; Pineda-García *et al.*, 2015; Powell *et al.*, 2017) or lower drought tolerance in late-successional species (Apgaua *et al.*, 2015; Schönbeck *et al.*, 2015). Independent of their successional classification, larger trees have the potential to mitigate drought effects through stem capacitance and access to deep soil water (Phillips *et al.*, 2003; Čermák *et al.*, 2007; Schwendenmann *et al.*, 2015).

Recent studies suggest that drought-induced mortality is most common at the end of the growth spectrum, with highest mortalities reported at the seedling stage and in large trees (Engelbrecht *et al.*, 2006; Nepstad *et al.*, 2007; Rowland *et al.*, 2015; Meakem *et al.*, 2017). In the moist lowland forests of Panama, transpiration in canopy trees is generally energy limited as a result of frequent cloud cover and abundant soil water content, especially during the rainy season (Graham *et al.*, 2003), and regulated by structural (leaf area) rather than physiological (stomatal control) means (Phillips *et al.*, 2001; Wolfe *et al.*, 2016). Understanding both plant hydraulic conductivity and response to environmental drivers is crucial to improve predictive understanding of drought responses. When soil-water and plant-water transport are non-limiting, transpiration is a function of available energy (radiation) and atmospheric dryness (vapor pressure deficit), i.e. atmospheric demand (Penman, 1948; Monteith, 1965). Diel transpiration is approximately linearly related to radiation or vapor pressure deficit – whichever is more limiting – until maximum hydraulic conductivity occurs and saturation of transpiration is reached (Oren *et al.*, 1999). Thus, deviations from these linear relationships can be indicative of regulatory responses, such as stomatal closure or hydraulic limitations, and statistical modeling of these deviations can be used to detect parameters that limit transpiration, such as soil volumetric water content (Oren *et al.*, 1998; Eller *et al.*, 2015). Moreover, time lags and hysteresis patterns in the diurnal relationship between transpiration, vapor pressure deficit, and photosynthetic photon flux density can be used to determine the biotic and abiotic factors that limit transpiration (O'Grady *et al.*, 1999; Phillips *et al.*, 1999; Matheny *et al.*, 2014; Zhang *et al.*, 2014; Mallick *et al.*, 2016). In addition, nocturnal sap flow can be an indicator of stem refilling of capacitance storage in drought-stressed trees (Pfautsch & Adams, 2013) and has been shown to be significantly higher in dry season compared to wet season periods in tropical biomes (Forster, 2014).

The main objective of this study is to elucidate the interactions between plant hydraulics, successional stage, and environmental drivers in species-diverse secondary tropical forests during the severe drought of the 2015/16 ENSO event in central Panama. Utilizing a chronosequence approach, we measured sap flow in 8-, 25-, and 80-year old secondary forests and tested the following hypotheses: (1) Early-successional forests exhibit highest overall sap velocities and sapwood-specific hydraulic conductivities due to typically higher leaf area allocation and leaf-level water demand of fast-growing, shade-intolerant pioneer species. (2) Early-successional forests experience reduced sap velocities during the dry-season drought, due to presumed shallower rooting depth in 8-year old trees compared to 80-year

old trees, and exhibit strong regulatory responses and opportunistic water use strategies. (3) Late-successional forests exhibit no decrease in sap velocities during drought periods due to presumed access to deep soil water reservoirs and stem water storage in larger trees. (4) Sap velocities in early-successional forests are mainly driven by radiation due to high exposure in a single-layered forest and prevalence of opportunistic pioneer species, whereas vapor pressure deficit is the main driver of sap velocities in late-successional forests due to the presence of a multi-layered, partially-shaded canopy with a higher proportion of shade-adapted species.

Materials and Methods

Study Area

All sites were located in the "Agua Salud Project" study area (AS), located centrally in the Panama Canal Watershed (PCW; 9°13' N, 79°47'W, 330 m a.s.l.). The study area borders Soberania National Park to the west and comprises a mosaic of land uses types that are typical for the PCW, including cattle pastures, fallows, timber plantations, and secondary forests patches. Local topography is characterized by rolling hills with steep slopes and a dense network of small streams. Soils are deep Oxisols with relatively low fertility (Turner & Engelbrecht, 2011). The climate is sub-humid tropical, with an annual mean precipitation of 2700 mm and a pronounced dry season from late-December to mid-May (Ogden *et al.*, 2013). In 2015, strong ENSO conditions resulted in only 1800 mm precipitation, and 2014-2016 marked the driest contiguous 3-year period since the beginning of instrumental data collection in 1925 on Barro Colorado Island, located ~12 km southwest from the study area (data provided by the Physical Monitoring Program of the Smithsonian Tropical Research Institute).

We used a chronosequence approach to monitor transpiration across a successional gradient in secondary forests throughout the 2015/16 ENSO event. Despite known limitations of chronosequence studies (Johnson & Miyanishi, 2008) and the reported uncertainties of successional trajectories in neotropical forest succession (Norden *et al.*, 2015), there is sufficient support to this approach in the literature. In the AS project area, early-successional forests are more similar to one another than late-successional forests, both in regards to composition (van Breugel *et al.*, 2013) and functional traits (Craven *et al.*, 2015). In addition, general trends in biophysical traits are largely independent of taxonomic affiliation and a tight link exists between these traits and water use strategies (Ewers *et al.*, 2011). We studied three stands of secondary forest including young (hereafter SF8 for secondary forest of 8 years age at the beginning of data collection), 25-year-old, and 80-year-old forest (hereafter SF25 and SF80). All three stands were utilized as a cattle pasture prior to stand initiation; basal area was 9.4, 16.0, and 31.5 $m^2\ h^{-1}$ in SF8, SF25, and SF80, respectively (Table S1; van Breugel *et al.*, 2013). Sap flow was measured on one hillslope each in SF8 and SF80, and two hillslopes in SF25 at the halfway point between

ridgetop and valley bottom, with total slope distances of 139, 103/104, and 60 m in SF8, SF25, and SF80, respectively. Slopes were 29, 29/33, and 24 degrees and aspects were 219, 242/70 and 202 degrees in SF8, SF25, and SF80, respectively. Elevations at the center of each sap flow site were 264, 276/246, and 190 m a.s.l. in SF8, SF25, and SF80, respectively.

Sap Flow Measurements

We used heat-ratio sap flow sensors (Marshall, 1958) to measure sap flow in 76 trees, representing 46 species, across all sites (Table S2). Initial tree selection was based on diameter at breast height (DBH) to represent local size distribution rather than species. In a landscape-scale study of forest succession in the AS project area, van Breugel *et al.* (2013) found that only six of the 526 plant species made up more than 5% of all plants ≥ 1 cm diameter in more than 10% of their 108 plots. Thus, most locally dominant species were not dominant across the metacommunity and selecting species based on local dominants can result in biased samples. We included small and understory trees to ensure adequate representation of establishing late-successional trees to capture a wider range of canopy positions, especially in older forests. Based on relative canopy position, 13 of the 27 instrumented trees in SF80 were classified as sub-canopy trees, compared to three and zero sub-canopy trees in SF25 and SF8, respectively. Lastly, tree size has been shown to be more important than species affiliation when determining sap velocities in a multi-species forest (Hernandez-Santana *et al.*, 2015; Moore *et al.*, 2017). All selected trees were identified to species level and compared to their local abundance based on basal area data from nearby secondary succession plots (van Breugel *et al.*, 2013). Based on these data, we identified two species in SF8 (*Conostegia xalapensis, Vismia macrophylla*) and two species in SF25 (*Xylopia frutescens, Vismia macrophylla*) that each account for at least 5% of basal area in all four and all three nearby secondary succession plots in SF8 and SF25, respectively. As a result, two additional individuals of *Conostegia xalapensis* and one individual of *Vismia macrophylla* were instrumented in SF8 to better represent these locally (pre-) dominant species, whereas *Xylopia frutescens* and *Vismia macrophylla* were already adequately represented in SF25 with 5 and 4 instrumented trees, respectively (Table S2). No dominant species were identified in SF80.

Sensors were installed at breast height (~1.37 m) on the upslope-facing side of the tree and were placed equidistantly from the heater using a drill guide. Despite potential radial variation in sap flow, we used one sensor per tree rather than multiple sensors per tree. Given a limited number of sensors, this approach has been shown to reduce uncertainties in estimates of stand-scale sap flow measurements (Komatsu *et al.*, 2017). Sensors were constructed using stainless steel hypodermic needles (1.3 mm diameter) cut to either 26 or 13 mm length. A copper-constantan thermocouple junction was inserted into the needle with an effective measurement depth of 20 mm (for use in trees with DBH > 5 cm) and 10 mm (for use in trees with DBH < 5 cm) for 26 and 13 mm needles, respectively. Heaters were constructed

using slightly larger needles (1.6 mm diameter) to accommodate constantan coils. All needles were sealed with epoxy at the tip and with hot glue at the fitting. To account for expectedly high flow rates, we chose a sensor spacing of 0.5 cm (Burgess *et al.*, 2001).

Data were logged in 30-minute intervals following a 3-second heat pulse and downloaded weekly beginning in 2015 on March 12 (SF25), May 21 (SF8), and July 29 (SF80) until August 31, 2016 (Table S3). To minimize noise and to allow for equilibration of temperature ratios (Burgess *et al.*, 2001), 20 measurements were logged and averaged after a 60-second delay following the pulse of heat. At each site, sensors were connected via differential channels to two AM16/32 multiplexers (Campbell Scientific, Logan, UT), controlled by a single CR1000 data logger (Campbell Scientific, Logan, UT). Measured temperature ratios were converted to heat pulse velocities V_h (cm h^{-1}) according Burgess *et al.* (2001):

$$V_h = \frac{k}{x} \ln\left(\frac{v_1}{v_2}\right) 3600\,, \qquad \text{Eqn 1}$$

where k is thermal diffusivity of wood ($cm^2\ s^{-1}$), x is the distance between heater and either sensor (cm), and v_1/v_2 is the temperature ratio between downstream and upstream sensor. V_h was corrected for wounding according to the numerical solution by Burgess *et al.* (2001) and converted to sap velocity V_s (cm h^{-1}; Marshall, 1958; Barrett *et al.*, 1995):

$$V_s = \frac{V_c \rho_b (c_w + m_c c_s)}{\rho_s c_s}\,, \qquad \text{Eqn 2}$$

where ρ_b is wood density (g cm^{-3}), c_w and c_s are specific heat capacities of wood and water (J kg^{-1} K^{-1}), respectively, m_c is water content of sapwood, and ρ_s in the density of water (g cm^{-3}). Wood properties of instrumented tree species were taken from a local dataset (Wright *et al.*, 2010). To account for potential probe misalignment, we induced zero-flow conditions by severing xylem vessels using a battery-powered oscillating saw (DeWALT, model DCS355D1). Incisions were 4 cm wide, 6 cm deep, and located 3 cm above and below sensors on a subset of trees with large enough diameters to reduce risk of wound-induced mortality. After validation of zero-flow, a new set of sensors was installed on the same tree. Zero-flow conditions were also assumed to occur pre-dawn (03:00-4:30) during periods with low atmospheric demand for water (VPD < 0.2 kPa). Data from induced zero-flow measurements were used to validate data from assumed zero-flow conditions. Of the 76 instrumented individuals, data from six individuals were excluded from the analysis due to mortality (four trees) and high noise levels in the data (two trees; Table S2). No gap filling was performed.

Micrometeorological Measurements

A meteorological station within the AS project area provided local climate data, including net radiation ($W \cdot m^{-2}$) using a CN4 net radiometer (Kipp & Zonen, Delft, Netherlands), air temperature (°C) and relative humidity (RH, %) using an HMP60 (Vaisala, Vantaa, Finland), photosynthetic photon flux density (PPFD, µmol m^{-2} s^{-1}) using a PSQ1 quantum sensor (Kipp & Zonen, Delft, Netherlands),

precipitation (mm) using a 260-250-A tipping bucket (NovaLynx, CA, USA), and wind speed (WS, m s^{-1}) using a 05103 wind anemometer (R. M. Young, Michigan, USA). Vapor pressure deficit (VPD, kPA) was calculated from these data following Allen *et al.* (1998). In each forest, soil volumetric water content (VWC) was measured in three locations along the hillslope using GS1 sensors (Decagon Devices, Pullman, WA) at three measurement depths (10, 30, and 50 cm) each. A single term for VWC was calculated, based on the weighted-by-depth average of data from 10, 30, and 50 cm depth.

Hydraulic Conductivity

Leaf water potentials Ψ_L were measured in the dry (March 6-16, 2016) and the wet season (July 26-28, 2016) using a pressure chamber (PMS Instrument Company, Albany, OR). In all forests, data were collected pre-dawn (3:00-5:00), midday (11:00-14:00), and pre-dusk (17:00-19:00). Data collection was limited to instrumented trees of which the canopy could be clearly distinguished from neighboring trees and that could be reached using 5 m long pole pruners (N_{SF8} = 7, N_{SF25} = 8, N_{SF80} = 11). To test for within-tree heterogeneity of Ψ_L, we sampled 36 leaves from different positions within the canopy (lower-canopy sun, lower-canopy shade, upper-canopy sun, upper-canopy shade) from nine trees representing eight species in SF80 using a sling shot at midday (11:00-13:00) during the dry season on February 22, 2017, when Ψ_L gradients in the canopy are likely most pronounced. Lower-canopy leaves were sampled between 2 to 5 m height, upper-canopy leaves were sampled between 15 and 25 m height. ANOVA results show no significant difference in Ψ_L at different canopy positions (p = 0.57, Figure S1), suggesting that lower canopy samples can be used as a proxy for average Ψ_L throughout the canopy. Similarly small gradients in Ψ_L have been found by Oberbauer *et al.* (1987) in Costa Rica.

Darcy's law approximated sapwood-specific conductivity K_s was calculated for each tree (Tyree & Ewers, 1991) from the slope parameter of simple linear-regression of sap flux density and leaf water potentials (Martínez-Vilalta *et al.*, 2014). Several assumptions are associated with this approach: First, we assumed homogeneous sap flow throughout the sapwood and accordingly calculated the volume of sap flowing across an area of sapwood based on conversion of V_s (cm h^{-1}) to sap flux density J (cm^3 m^{-1} s^{-1}). Second, we assume that Ψ_L measurements are representative of average canopy Ψ_L (see above). Third, the approach accounts for the assumptions of obtaining Ψ_L at true peak sap flow and uncertainties of equilibration of soil water potential Ψ_S and Ψ_L at predawn (Martínez-Vilalta *et al.*, 2014; Hochberg *et al.*, 2017). Lastly, to account for vertical heterogeneity in V_s (i.e. stem hydraulic capacitance), we used sap flow data at the timestamp with the highest correlation coefficient between evaporative demand and up to 90-minutes time-lagged sap flow rates on the day of water potential measurements for each tree. Evaporative demand (m s^{-1}) was calculated according Van Bavel (1966) and Bladon *et al.* (2006).

$$ET_p = \frac{\Delta Q^* + \rho_a c_a u D}{\rho_\omega \lambda_v (\Delta + \gamma)}, \quad \text{Eqn 3}$$

where Δ is the slope of the saturation vapor pressure curve (Pa K^{-1}), Q* is net radiation (J m^{-2} s^{-1}), ρ_a is density of air (kg m^{-3}), c_a is heat capacity of air (J kg^{-1} K^{-1}), u is wind speed (m s^{-1}), D is vapor pressure deficit (Pa), ρ_ω is density of water (kg m^{-1}), λ_υ is the latent heat of vaporization (J kg^{-1}), and γ is the psychrometric constant (Pa K^{-1}). A total of 203 measurements were included in the analysis and resulting K_s values were averaged by forest age.

Statistical Analysis

Due to the robustness of linear mixed models in dealing with longitudinal data with missing data as well as temporal autocorrelation (von Ende, 2001), a linear mixed model (M-1) was used to assess differences in average seasonal V_s or K_s (response) between seasons, forest age, and the interaction between season and forest age (fixed effects), while accounting for individual trees (random effect). Seasons were classified according to official dates provided by the Meteorological and Hydrological Branch of the Panama Canal Authority, with the wet seasons starting on May 17 (2015) and April 27 (2016), and the dry seasons starting on November 27 (2015) and December 19 (2016). Analysis was limited to a subset of trees for which data were available in all seasons (N_{SF8} = 15, N_{SF25} = 25, N_{SF80} = 26). Differences of V_s and K_s between seasons for a given forest age were assessed via least square means pairwise comparisons. One-sample t-tests were used to test whether nocturnal flow was significantly different from zero for each forest and season. Where multiple tests were performed, the Bonferroni correction was applied to account for multiple comparisons. A second linear measure mixed model (M-2) was used to assess differences in the effects of VPD, PPFD, WS, Precip., and VWC on average daily V_s between forest ages, accounting for random effects of seasons and individual trees. Despite the known interaction between VPD and PPFD (i.e. evaporative demand; Eqn 3) and their separate mechanistic impacts on transpiration (Bladon *et al.*, 2006), we chose to separate these parameters to be able to test for potential differences due to successional shifts in shade tolerance and a canopy structure. Model parameters were statistically evaluated using the Markov Chain Monte Carlo method with 1000 iterations (R-package "MCMCglmm"; Hadfield, 2010). For comparative analyses between forest ages using models M-1 and M-2, data were limited to July 29, 2015 to August 31, 2016 when data were collected in all forests. Wood densities were assessed for differences between forests via ANOVA. Differences in Ψ_L and soil VWC between forests were assessed via linear mixed models and least square means pairwise comparisons. Mixed effect model analyses were performed using the R-package “lme4” (Bates *et al.*, 2014) and pairwise comparisons using the R-package “multcomp” (Hothorn *et al.*, 2008).

A linear regression model was developed with VPD, PPFD, WS, Prec., and VWC as predictors and average daily V_s across trees per forest age as response. To minimize within-forest variance, the relationship between standard deviation of daily mean V_s and sample size was assessed (Figure S2). Subsequently, only days with data from at least 10 (SF8 & SF25) or 15 (SF80) trees were included in the

analysis. Linear regression models were based on Box-Cox transformed data beginning from the earliest time of measurement in each forest (Box & Cox, 1964). Relative importance metrics of environmental predictors were calculated (R-package "relaimpo"; Grömping, 2006), including each predictor's usefulness (model contribution given all other predictor already included in the model) and overall model contribution averaged over orderings of predictors (Chevan & Sutherland, 1991). To account for a potential size-effect, we performed a separate analysis of relative importance metrics on a subset of trees smaller than 15 cm DBH in SF25 and SF80. Confidence intervals for relative importance metrics were calculated via bootstrapping (1000 runs). All data processing and analyses were performed in R 3.3.2 (R Core Team, 2015).

Results

Diel patterns of V_s closely follow VPD and PPFD in all forests, with V_s lagging slightly behind PPFD in SF8 and SF80, but not in SF25 (Fig. 1). In all forests, a clockwise hysteresis is evident between normalized half-hourly V_s and VPD, especially during the dry season, and a counter-clockwise hysteresis is evident in the relationship between V_s and PPFD, especially in SF8 and SF80 (Fig. 2). Average Ψ_L during the dry season was similar among forests, ranging from -0.4 to -0.6 and from -1.6 to -1.7 MPa at pre-dawn and midday, respectively (Fig. 3a). Pre-dusk Ψ_L was significantly less negative in SF8 than SF80 ($p = 0.04$), with -0.9 and -1.4 MPa, respectively. In the wet season, average Ψ_L was similar among all forests, ranging from -0.3 to -0.4 and from -0.4 to -0.5 MPa at pre-dawn and pre-dusk, respectively (Fig. 3b). Midday Ψ_L was significantly less negative in SF80 compared to SF8 ($p < 0.001$) and SF25 ($p = 0.018$), with -0.4, -0.7, and -0.9 MPa, respectively. Significant night-time sap flow occurred during the dry season in SF25 (2.01 cm h^{-1}; $p = 0.002$) and SF80 (1.90 cm h^{-1}; $p < 0.001$), reaching 11% and 8.7% of average daytime V_s in SF25 and SF80, respectively (Table 1). Night-time flow was not significant in SF8 or during wet season periods in any forest.

Seasonality had a significant effect on V_s, as reflected in clear seasonal patterns across all forests (M-1, $p < 0.001$; Table 2, Fig. 4). Although average V_s tended to be highest in SF8 and decreased with increasing forest age, the differences among forests are non-significant (Table 2, Fig. 5). In SF80, average V_s was significantly higher in the dry season compared to both wet seasons ($p < 0.01$), whereas no significant differences between seasons were detected in SF8 and SF25 (Table 2). Seasonality also had a significant effect on K_s ($p = 0.013$). In July 2016 (wet season), K_s values were 5.81 ± 2.14, 5.22 ± 2.2, and 1.75 ± 1.3 mol m^{-2} s^{-1} MPa^{-1} in SF8, SF25, and SF80, respectively (Fig. 6). Compared to wet season values, K_s in the dry season (March 2016) decreased significantly by 69% ($p = 0.013$) and 75% ($p < 0.001$) to 1.8 ± 1.17 and 1.3 ± 0.42 mol m^{-2} s^{-1} MPa^{-1} in SF8 and SF25, respectively. In SF80, the wet-to-dry-season increase of K_s by 5% to 1.84 ± 0.44 mol m^{-2} s^{-1} MPa^{-1} was not significant. Wood densities

were not significantly different between forests ($p = 0.06$), with mean and standard error values of 0.59 ± 0.02, 0.53 ± 0.02, and 0.59 ± 0.02 g cm^{-3} in SF8, SF25, and SF80, respectively.

When accounting for seasonal and daily variance (M-2), significant differences in age-specific behavior and responses to environmental variables were detected. All environmental main effects (VPD, PPFD, WS, Precip., VWC) and the interactions between forest age and VPD, PPFD, WS, and VWC are significant (Table S4). Model parameter estimates suggest that VPD was a strong driver of V_s in all forests, with slopes of 3.81, 4.74, and 5.58 in SF8, SF25, and SF80, respectively. Precipitation is the only main effect with a negative slope parameter (-0.05). The effect of VPD on V_s was significantly greater in SF80 than in SF8 and the effect of PPFD was significantly greater in both SF8 and SF25 compared to SF80. WS had a significantly greater effect on V_s in SF25 compared to both SF8 and SF80. Soil VWC parameter estimates are significantly different between all forests and are the only model parameters with changing signs, with positive slopes for SF8 (0.2) and SF25 (0.08) and a negative slope for SF80 (-0.11).

Single-variable linear regression of VPD and V_s explains 48%, 54%, and 71% in SF8, SF25, and SF80, respectively (Fig. 7a,c,e). In SF8 and SF25, residuals show a distinct pattern when plotted against VWC below 40% (Fig. 7b,d,f). Below this threshold, VWC explains 42% ($p < 0.001$) and 7% ($p < 0.001$) of the residuals in SF8 and SF25, respectively, whereas no significant relationship between residuals and VWC was detected in SF80. Single-variable regression of PPFD and V_s explained 60%, 59%, and 66% in SF8, SF25, and SF80, respectively, with similar relationships between residuals and VWC as above (Figure S3). The proportion of variance explained by linear regression including all predictors is 69%, 66%, and 86% in SF8, SF25, and SF80, respectively. Overall model contributions averaged over orderings of predictors show PPFD and VPD as the main drivers of V_s, together accounting for 77%, 71%, and 63% of model strength in SF8, SF25, and SF80, respectively (Table 3). With progressing forest age, VPD replaces PPFD as primary driver of V_s. Parameter usefulness of WS increases with increasing forest age from 3% in SF8, to 12% and 13% in SF25 and SF80, respectively, whereas parameter usefulness of VWC decreases from 31% in SF8 to 11% and 4% in SF25 and SF80, respectively (Table 3).

Of the species that were classified as deciduous or semi-deciduous (Table S2), most exhibited only brief periods of dormancy at varying times throughout the year. However, the simultaneous, prolonged dormancy of four *Annona spraguei* and one *Casearia arborea* caused a sharp decline in average V_s in SF25 at the dry-wet transition in April 2016 (Fig. 4). Excluding aforementioned trees from the analysis resulted in a less dramatic drop and overall higher V_s at the end of the dry season in SF25 (Figure S4), improved linear regression model performance in SF25 to 72%, and reduced parameter usefulness of VWC to 2% (Table S6).

Discussion

Differences along the Chronosequence

Our results show that tropical secondary forests in central Panama exhibited different seasonal behavior and response to drought-induced water limitations during the 2015/2016 ENSO event, with clear differences along the successional gradient. Amidst species-specific differences in hydraulic architecture, early-successional and light-demanding species are generally characterized by low wood densities and wide vessel diameters, resulting in higher hydraulic conductivity and transpiration rates that facilitate their typical fast growth behavior (Finegan, 1984; Granier *et al.*, 1996; Tyree *et al.*, 1998; Sack *et al.*, 2005; Poorter *et al.*, 2010). Forests in the AS project area reflect these patterns as they exhibit a shift of functional strategies from resource acquisition to resource conservation with progressing succession (Craven *et al.*, 2015). Although the observed differences in V_s and K_s between forest ages are non-significant and thus fail to support the first hypothesis – higher overall V_s and K_s due to higher water demands early-successional forests – our data agree with aforementioned general trends as average V_s as well as K_s during the wet season decrease with progressing forest age (Fig. 5). The lack of significant differences in V_s between forests can in part be attributed to similar wood densities of instrumented trees in all forests, suggesting similar hydraulic architecture (Santiago *et al.*, 2004), as well as the strong seasonal, inversely-phased fluctuations in V_s between forest ages (Fig. 4). Including additional trees from mature or primary forest to the chronosequence would further clarify if the hypothesized trend is found along a broader successional gradient.

Our results partially lend support to the second hypothesis, that water use is reduced in early-successional forest during the 2015/16 ENSO dry-season drought. Pronounced hysteresis loops, differences in Ψ_L, and significant reductions in K_s during the dry season (Fig. 2, Fig. 3a, Fig. 5) suggest stomatal regulation to prevent hydraulic failure in SF8 and SF25. Although K_s measurements are associated with uncertainties due to potential species-specific structural differences, K_s was not significantly related to wood density, thus further supporting environmental factors as drivers of observed differences. Similar to our study, Huc *et al.* (1994) found that early-successional tropical rainforest species in French Guiana exhibit significantly decreased stomatal and plant-intrinsic hydraulic conductances and less negative midday Ψ_L whereas late-successional species exhibit no change in the dry season. Although increasingly becoming the subject of debate (Hochberg *et al.*, 2017), isohydric behavior, i.e. maintenance of constant Ψ_L through regulation of stomatal conductance, is a typical drought avoidance strategy (Bucci *et al.*, 2005) and has been shown to be predominantly a trait in pioneer and early-successional species in a tropical dry forest in Bolivia (Markesteijn *et al.*, 2011). In central Panama, drought-intolerant species are associated with little tolerance to low leaf water status and relatively higher hydraulic stem conductances (Kursar *et al.*, 2009). Thus, although we did not directly assess drought

tolerance by means of mortality or percent loss of hydraulic conductivity, the greater response to soil VWC in SF8 (Fig. 7, Table 3) suggests that trees in early-successional forests experienced more drought stress than trees in late-successional forests, and consequently regulated water use during the 2015/16 ENSO dry-season drought.

The third hypothesis, that late-successional forests do not limit water use during the 2015/16 ENSO dry-season drought, was supported by our data (Fig. 5A). Studies on seasonal differences of transpiration in tropical forests report inconsistent results, including higher whole-tree transpiration in the dry season (Meinzer *et al.*, 1999; O'Grady *et al.*, 1999; Schwendenmann *et al.*, 2015), similar canopy transpiration between seasons (Kumagai *et al.*, 2004), or higher stand transpiration in the wet season (McJannet *et al.*, 2007), suggesting complex interactions between taxonomic, physiognomic, microclimatic, edaphic, and topographic factors. Canopy trees in Panama have been shown to exhibit little stomatal control and CO_2 uptake is limited by light rather than water during the wet season (Phillips *et al.*, 2001; Graham *et al.*, 2003). In our study, V_s increased considerably in all forests at the beginning of the dry season when soils are still water-saturated and cloud cover is low, lending support to light as the limiting factor of transpiration (Fig. 4). Several studies have found direct or indirect evidence that trees with access to deep soil water maintain a favorable plant water status and higher transpiration throughout periods of reduced moisture availability (Jackson *et al.*, 1995; Jackson *et al.*, 1999; Meinzer *et al.*, 1999; Stahl *et al.*, 2013; Schwendenmann *et al.*, 2015). In Panama, trees and lianas in old-growth forest utilize a higher proportion of deeper soil water at the end of the dry season (Andrade *et al.*, 2005). Although root architecture varies considerably by species in Panama, with some species allocating significantly more resources to tap roots compared to lateral roots (Sinacore *et al.*, 2017), it can safely be assumed that long-established trees in SF80 have deeper, larger root systems compared to younger trees in SF8, providing one explanation for sustained higher V_s during the dry season in SF80. Despite clear evidence for differences in behavior with forest age during the 2015/16 ENSO drought, long-term data are required to elucidate whether observed differences between forests are a direct result of the drought or fall within the typical seasonal behavior.

Trees in Panama exhibit considerable stem water storage capacitance that is linearly related to sapwood area, with 10 kg of stored water per 0.1 m^2 sapwood area (Goldstein *et al.*, 1998). The significant nocturnal sap flow observed in SF25 and SF80 during the dry season, when VPD was comparatively low, could be indicative of stem refilling in large trees with greater stem water capacitance (Forster, 2014). However, the benefits of stem water storage could be size-independent, as stored stem water improved the tolerance to soil drought of only 1-year old late-successional species of a tropical dry forest in Mexico (Pineda-Garcia *et al.*, 2012), and had similar potential to alleviate hydraulic constraints in small and large trees in Panama (Phillips *et al.*, 2001). More research on whether stem capacitance has

a disproportionally greater effect on drought avoidance in large trees compared to small trees is required, such as simultaneous measurements of canopy conductance as well as sap flow at different heights in the stem and branches (Meinzer *et al.*, 2004) and in roots across the chronosequence.

Environmental Drivers

Our data lend support to the fourth hypothesis, that VPD replaces PPFD as the main driver of V_s in late-successional forests (Table 3). Light availability in the understory of secondary forest in Panama is reduced to less than 10% of above-canopy values after 20 years of growth (van Breugel *et al.*, 2013). Consequently, the proportion of species with low light saturation points increases with progressing forest succession. As these species are adapted to low light conditions, VPD rather than PPFD becomes the primary limiting factor of transpiration in late-successional forests, making it one of the biological mechanisms that cause a feedback between microclimate and succession (Lebrija-Trejos *et al.*, 2011).

Taller canopies are generally more exposed to wind and thus better coupled to the atmosphere (Jarvis, 1984). In addition, transpiration in well-coupled canopies is mainly driven VPD rather than radiation (Jarvis, 1984; Zhang *et al.*, 2014). The increasing relative importance of WS with progressing forest age paired with the higher sensitivity of V_s to VPD suggest a higher degree of canopy coupling in older forests due to increasing height. This is further supported by the smaller magnitude of the hysteresis between V_s and VPD in SF80 compared to SF8 and SF25, indicating that V_s is largely in phase with VPD in SF80. Estimates of omega decoupling coefficients (Jarvis, 1984) agree with this trend, with highest decoupling coefficients in SF8 and lowest in SF80 (Figure S5).

The negative effect of precipitation on V_s is likely linked to leaf wetness, which had a strong inhibitory effect on sap flow in a tropical could forest tree in Brazil (Eller *et al.*, 2015) and reduced transpiration by up to 28% in a tropical moist forest in central Costa Rica (Aparecido *et al.*, 2016). In the AS project area, canopy interception values approach levels of mature lowland forests after approximately 10 years of growth (Zimmermann *et al.*, 2013), explaining the observed significant difference in the effect of precipitation between SF8 and SF80. The counterclockwise hysteresis between PPFD and V_s in all forests, specifically the morning lag, could be indicative of either stem capacitance or the inhibition of diffusion due to leaf wetness from dew that accumulated on the leaves at night (O'Brien *et al.*, 2004).

The different effect of soil VWC on V_s between forests indicates that trees in SF8 and SF25 experience some degree of water limitation, whereas higher soil VWC had a negative effect on V_s in SF80. Soil VWC in SF80 remained comparatively wet throughout the dry season, never dropping below 35% (Fig. 7f, Fig. 8). If soil VWC remains well above the threshold for trees to maintain a favorable plant water status, increases in soil VWC beyond that point will have no positive effect on V_s but instead have the potential to reduce V_s as increases in VWC coincide with leaf-wetting precipitation events. The difference in soil VWC during the dry season between forests (Fig. 8) could be indicative of a higher

proportion of deep water usage of trees in SF80. Although not directly tested in this study, hydraulic redistribution by larger trees can relocate water from deep to more shallow soil layers, potentially facilitating water access of understory trees (Dawson, 1996; Caldwell *et al.*, 1998; Oliveira *et al.*, 2005). The observed difference in soil VWC data during the dry season drought, paired with our sap flow data, indicate a feedback effect between soil properties and succession that has the potential to alleviate drought severity in older regrowing secondary forests in central Panama. Furthermore, soil water availability is a direct determinant of local and regional species distribution in tropical forest of Panama, and even short dry-spells can cause significant mortality in establishing seedlings (Engelbrecht *et al.*, 2006; Engelbrecht *et al.*, 2007). Water stress is a major factor in shaping geographic distributions of large trees in Panama (Meakem *et al.*, 2017). Contrary to SF8, both SF25 and SF80 have previously experienced droughts, including the severe 1997/1998 (SF25 & SF80) and 1982/1983 ENSO (SF80) events, potentially shifting species composition towards more drought-tolerant species in the older forests.

Conclusion

Our study shows that trees in early-successional forests displayed stronger signs of regulatory responses to the 2015/16 ENSO drought, and that the limiting physiological processes for V_s shift from operating at the plant-soil interface to the plant-atmosphere interface with progressing forest succession, likely as a result of favorable soil characteristics and access to deeper soil water in late-successional forests. Knowledge of the resilience of establishing secondary forests to drought is not only important for optimizing reforestation efforts but also for development and optimization of models to predict water and carbon fluxes in a dynamic landscape that comprises a mosaic of pastures and forest fragments at different successional stages.

Acknowledgements

This work is a contribution of the Agua Salud Project of the Smithsonian Tropical Research Institute (STRI). Agua Salud is part of ForestGEO and is a collaboration with the Panama Canal Authority (ACP), the Ministry of the Environment (MiAmbiente) of Panama, and other partners. The authors thank Fred Ogden, Edward Kempema, Daniel Beverly, Jazlyn Hall (University of Wyoming), Robert Stallard, Holly Barnard (University of Colorado), Steven Paton, Alicia Entem, Estrella Yanguas, Anabel Rivas, and Adriana Tapia (STRI) for their significant contribution to this study. For their help in the field and laboratory, we thank Sergio Dos Santos, Federico Davies, Mario Bailon, Andres Hernandez, Joana Balbuena, Eric Diaz, Guillermo Fernandez, Arnulfo Hernandez, Jorge Batista, Adam Bouché, Laura Lyon, Joan Herrmann, Catalina Guerra, Emily Purvis, Katherine Sinacore, Ethan Miller, Heather Speckman, and John Frank. Funding for this research was provided by the U.S. National Science

488 Foundation (NSF) EAR-1360384, Stanley Motta, the Silicon Valley Foundation, and the Heising-Simons
489 Foundation.

490 **Author Contribution**

491 M.B., B.E.E., and J.S.H. designed the study. M.B. collected data; M.B. carried out data analysis
492 with input from B.E.E.; M.B. wrote the manuscript with revisions by all coauthors.
493

References

Allen RG, Pereira LS, Raes D, Smith M. 1998. Crop evapotranspiration-Guidelines for computing crop water requirements-FAO Irrigation and drainage paper 56. *FAO, Rome* **300**(9): D05109.

Andrade JL, Meinzer FC, Goldstein G, Schnitzer SA. 2005. Water uptake and transport in lianas and co-occurring trees of a seasonally dry tropical forest. *Trees* **19**(3): 282-289.

Aparecido LMT, Miller GR, Cahill AT, Moore GW. 2016. Comparison of tree transpiration under wet and dry canopy conditions in a Costa Rican premontane tropical forest. *Hydrological Processes* **30**(26): 5000-5011.

Apgaua DM, Ishida FY, Tng DY, Laidlaw MJ, Santos RM, Rumman R, Eamus D, Holtum JA, Laurance SG. 2015. Functional traits and water transport strategies in lowland tropical rainforest trees. *PLoS One* **10**(6): e0130799.

Barrett D, Hatton T, Ash J, Ball M. 1995. Evaluation of the heat pulse velocity technique for measurement of sap flow in rainforest and eucalypt forest species of south-eastern Australia. *Plant, Cell & Environment* **18**(4): 463-469.

Bates D, Mächler M, Bolker B, Walker S. 2014. Fitting linear mixed-effects models using lme4. *arXiv preprint arXiv:1406.5823*.

Bazzaz F, Pickett S. 1980. Physiological ecology of tropical succession: a comparative review. *Annual review of ecology and systematics* **11**: 287-310.

Bladon KD, Silins U, Landhäusser SM, Lieffers VJ. 2006. Differential transpiration by three boreal tree species in response to increased evaporative demand after variable retention harvesting. *Agricultural and Forest Meteorology* **138**(1): 104-119.

Box GE, Cox DR. 1964. An analysis of transformations. *Journal of the Royal Statistical Society. Series B (Methodological)* **26**(2): 211-252.

Bucci SJ, Goldstein G, Meinzer FC, Franco AC, Campanello P, Scholz FG. 2005. Mechanisms contributing to seasonal homeostasis of minimum leaf water potential and predawn

519 disequilibrium between soil and plant water potential in Neotropical savanna trees. *Trees* **19**(3):
520 296-304.
521 **Burgess SS, Adams MA, Turner NC, Beverly CR, Ong CK, Khan AA, Bleby TM. 2001.** An
522 improved heat pulse method to measure low and reverse rates of sap flow in woody plants. *Tree*
523 *Physiology* **21**(9): 589-598.
524 **Caldwell MM, Dawson TE, Richards JH. 1998.** Hydraulic lift: consequences of water efflux from the
525 roots of plants. *Oecologia* **113**(2): 151-161.
526 **Čermák J, Kučera J, Bauerle WL, Phillips N, Hinckley TM. 2007.** Tree water storage and its diurnal
527 dynamics related to sap flow and changes in stem volume in old-growth Douglas-fir trees. *Tree*
528 *Physiology* **27**(2): 181-198.
529 **Chevan A, Sutherland M. 1991.** Hierarchical partitioning. *The American Statistician* **45**(2): 90-96.
530 **Craven D, Hall JS, Berlyn GP, Ashton MS, van Breugel M. 2015.** Changing gears during succession:
531 shifting functional strategies in young tropical secondary forests. *Oecologia* **179**(1): 293-305.
532 **Dawson TE. 1996.** Determining water use by trees and forests from isotopic, energy balance and
533 transpiration analyses: the roles of tree size and hydraulic lift. *Tree Physiology* **16**(1-2): 263-272.
534 **Eller CB, Burgess SS, Oliveira RS. 2015.** Environmental controls in the water use patterns of a tropical
535 cloud forest tree species, Drimys brasiliensis (Winteraceae). *Tree Physiology* **35**(4): 387-399.
536 **Engelbrecht BM, Comita LS, Condit R, Kursar TA, Tyree MT, Turner BL, Hubbell SP. 2007.**
537 Drought sensitivity shapes species distribution patterns in tropical forests. *Nature* **447**(7140): 80-
538 82.
539 **Engelbrecht BM, Dalling JW, Pearson TR, Wolf RL, Galvez DA, Koehler T, Tyree MT, Kursar**
540 **TA. 2006.** Short dry spells in the wet season increase mortality of tropical pioneer seedlings.
541 *Oecologia* **148**(2): 258-269.
542 **Escudero A, Valladares F. 2016.** Trait-based plant ecology: moving towards a unifying species
543 coexistence theory. *Oecologia* **180**(4): 919-922.

Ewers BE, Bond-Lamberty B, Mackay DS 2011. Consequences of stand age and species' functional trait changes on ecosystem water use of forests. *Size-and Age-Related Changes in Tree Structure and Function*: Springer, 481-505.

Finegan B. 1984. Forest succession. *Nature* **312**(8): 109-114.

Forster MA. 2014. How significant is nocturnal sap flow? *Tree Physiology* **34**(7): 757-765.

Goldstein G, Andrade J, Meinzer F, Holbrook N, Cavelier J, Jackson P, Celis A. 1998. Stem water storage and diurnal patterns of water use in tropical forest canopy trees. *Plant, Cell & Environment* **21**(4): 397-406.

Graham EA, Mulkey SS, Kitajima K, Phillips NG, Wright SJ. 2003. Cloud cover limits net CO2 uptake and growth of a rainforest tree during tropical rainy seasons. *Proceedings of the National Academy of Sciences* **100**(2): 572-576.

Granier A, Huc R, Barigah S. 1996. Transpiration of natural rain forest and its dependence on climatic factors. *Agricultural and Forest Meteorology* **78**(1-2): 19-29.

Grömping U. 2006. Relative importance for linear regression in R: the package relaimpo. *Journal of Statistical Software* **17**(1): 1-27.

Hadfield JD. 2010. MCMC methods for multi-response generalized linear mixed models: the MCMCglmm R package. *Journal of Statistical Software* **33**(2): 1-22.

Hansen J, Sato M. 2016. Regional climate change and national responsibilities. *Environmental Research Letters* **11**(3): 034009.

Hernandez-Santana V, Hernandez-Hernandez A, Vadeboncoeur MA, Asbjornsen H. 2015. Scaling from single-point sap velocity measurements to stand transpiration in a multispecies deciduous forest: uncertainty sources, stand structure effect, and future scenarios. *Canadian Journal of Forest Research* **45**(11): 1489-1497.

Hochberg U, Rockwell FE, Holbrook NM, Cochard H. 2017. Iso/Anisohydry: A Plant–Environment Interaction Rather Than a Simple Hydraulic Trait. *Trends in Plant Science* **23**(2): 112-120.

Hothorn T, Bretz F, Westfall P. 2008. Simultaneous inference in general parametric models. *Biometrical Journal* **50**(3): 346-363.

Huc R, Ferhi A, Guehl J. 1994. Pioneer and late stage tropical rainforest tree species (French Guiana) growing under common conditions differ in leaf gas exchange regulation, carbon isotope discrimination and leaf water potential. *Oecologia* **99**(3-4): 297-305.

Jackson P, Cavelier J, Goldstein G, Meinzer F, Holbrook N. 1995. Partitioning of water resources among plants of a lowland tropical forest. *Oecologia* **101**(2): 197-203.

Jackson PC, Meinzer FC, Bustamante M, Goldstein G, Franco A, Rundel PW, Caldas L, Igler E, Causin F. 1999. Partitioning of soil water among tree species in a Brazilian Cerrado ecosystem. *Tree Physiology* **19**(11): 717-724.

Jarvis P 1984. Coupling of transpiration to the atmosphere in horticultural crops: the omega factor. *I International Symposium on Water Relations in Fruit Crops 171*. 187-206.

Johnson EA, Miyanishi K. 2008. Testing the assumptions of chronosequences in succession. *Ecology Letters* **11**(5): 419-431.

Komatsu H, Kume T, Shinohara Y. 2017. Optimal sap flux sensor allocation for stand transpiration estimates: a non-dimensional analysis. *Annals of Forest Science* **74**(2): 38.

Kumagai To, Saitoh TM, Sato Y, Morooka T, Manfroi OJ, Kuraji K, Suzuki M. 2004. Transpiration, canopy conductance and the decoupling coefficient of a lowland mixed dipterocarp forest in Sarawak, Borneo: dry spell effects. *Journal of hydrology* **287**(1): 237-251.

Kunert N, Schwendenmann L, Hölscher D. 2010. Seasonal dynamics of tree sap flux and water use in nine species in Panamanian forest plantations. *Agricultural and Forest Meteorology* **150**(3): 411-419.

Kursar TA, Engelbrecht BM, Burke A, Tyree MT, EI Omari B, Giraldo JP. 2009. Tolerance to low leaf water status of tropical tree seedlings is related to drought performance and distribution. *Functional Ecology* **23**(1): 93-102.

Lebrija-Trejos E, Pérez-García EA, Meave JA, Poorter L, Bongers F. 2011. Environmental changes during secondary succession in a tropical dry forest in Mexico. *Journal of Tropical Ecology* **27**(05): 477-489.

Luo Z, Guan H, Zhang X, Zhang C, Liu N, Li G. 2016. Responses of plant water use to a severe summer drought for two subtropical tree species in the central southern China. *Journal of Hydrology: Regional Studies* **8**: 1-9.

Mallick K, Trebs I, Boegh E, Giustarini L, Schlerf M, Drewry DT, Hoffmann L, Randow Cv, Kruijt B, Araùjo A. 2016. Canopy-scale biophysical controls of transpiration and evaporation in the Amazon Basin. *Hydrology and Earth System Sciences* **20**(10): 4237-4264.

Markesteijn L, Poorter L, Bongers F, Paz H, Sack L. 2011. Hydraulics and life history of tropical dry forest tree species: coordination of species' drought and shade tolerance. *New Phytologist* **191**(2): 480-495.

Marshall D. 1958. Measurement of sap flow in conifers by heat transport. *Plant Physiology* **33**(6): 385.

Martínez-Vilalta J, Poyatos R, Aguadé D, Retana J, Mencuccini M. 2014. A new look at water transport regulation in plants. *New Phytologist* **204**(1): 105-115.

Matheny AM, Bohrer G, Vogel CS, Morin TH, He L, Frasson RPdM, Mirfenderesgi G, Schäfer KV, Gough CM, Ivanov VY. 2014. Species-specific transpiration responses to intermediate disturbance in a northern hardwood forest. *Journal of Geophysical Research: Biogeosciences* **119**(12): 2292-2311.

McGill BJ, Enquist BJ, Weiher E, Westoby M. 2006. Rebuilding community ecology from functional traits. *Trends in ecology & evolution* **21**(4): 178-185.

McJannet D, Fitch P, Disher M, Wallace J. 2007. Measurements of transpiration in four tropical rainforest types of north Queensland, Australia. *Hydrological Processes* **21**(26): 3549-3564.

Meakem V, Tepley AJ, Gonzalez-Akre EB, Herrmann V, Muller-Landau HC, Wright SJ, Hubbell SP, Condit R, Anderson-Teixeira KJ. 2017. Role of tree size in moist tropical forest carbon cycling and water deficit responses. *New Phytologist*.

Meinzer F, Goldstein G, Andrade J. 2001. Regulation of water flux through tropical forest canopy trees: do universal rules apply? *Tree Physiology* **21**(1): 19-26.

Meinzer FC, Andrade JL, Goldstein G, Holbrook NM, Cavelier J, Wright SJ. 1999. Partitioning of soil water among canopy trees in a seasonally dry tropical forest. *Oecologia* **121**(3): 293-301.

Meinzer FC, James SA, Goldstein G. 2004. Dynamics of transpiration, sap flow and use of stored water in tropical forest canopy trees. *Tree Physiology* **24**(8): 901-909.

Monteith JL 1965. Evaporation and environment. *The State and Movement of Water in Living Organisms, Proc. 19th Symp.* Swansea, U.K.: Society of Experimental Biology: Cambridge University Press. 205-234.

Moore GW, Orozco G, Aparecido LM, Miller GR. 2017. Upscaling transpiration in diverse forests: Insights from a tropical premontane site. *Ecohydrology*: 10.1002/eco.1920.

Nepstad DC, Tohver IM, Ray D, Moutinho P, Cardinot G. 2007. Mortality of large trees and lianas following experimental drought in an Amazon forest. *Ecology* **88**(9): 2259-2269.

Norden N, Angarita HA, Bongers F, Martínez-Ramos M, Granzow-de la Cerda I, Van Breugel M, Lebrija-Trejos E, Meave JA, Vandermeer J, Williamson GB. 2015. Successional dynamics in Neotropical forests are as uncertain as they are predictable. *Proceedings of the National Academy of Sciences* **112**(26): 8013-8018.

O'Brien JJ, Oberbauer SF, Clark DB. 2004. Whole tree xylem sap flow responses to multiple environmental variables in a wet tropical forest. *Plant, Cell & Environment* **27**(5): 551-567.

O'Grady A, Eamus D, Hutley L. 1999. Transpiration increases during the dry season: patterns of tree water use in eucalypt open-forests of northern Australia. *Tree Physiology* **19**(9): 591-597.

Oberbauer SF, Strain BR, Riechers G. 1987. Field water relations of a wet-tropical forest tree species, Pentaclethra macroloba (Mimosaceae). *Oecologia* **71**(3): 369-374.

Ogden FL, Crouch TD, Stallard RF, Hall JS. 2013. Effect of land cover and use on dry season river runoff, runoff efficiency, and peak storm runoff in the seasonal tropics of Central Panama. *Water resources research* **49**(12): 8443-8462.

Oliveira RS, Dawson TE, Burgess SS, Nepstad DC. 2005. Hydraulic redistribution in three Amazonian trees. *Oecologia* **145**(3): 354-363.

Oren R, Ewers BE, Todd P, Phillips N, Katul G. 1998. Water balance delineates the soil layer in which moisture affects canopy conductance. *Ecological Applications* **8**(4): 990-1002.

Oren R, Phillips N, Ewers B, Pataki D, Megonigal J. 1999. Sap-flux-scaled transpiration responses to light, vapor pressure deficit, and leaf area reduction in a flooded Taxodium distichum forest. *Tree Physiology* **19**(6): 337-347.

Penman HL 1948. Natural evaporation from open water, bare soil and grass. *Proceedings of the Royal Society of London A: Mathematical, Physical and Engineering Sciences*: The Royal Society. 120-145.

Pfautsch S, Adams MA. 2013. Water flux of Eucalyptus regnans: defying summer drought and a record heatwave in 2009. *Oecologia* **172**(2): 317-326.

Phillips N, Bond BJ, Ryan MG. 2001. Gas exchange and hydraulic properties in the crowns of two tree species in a Panamanian moist forest. *Trees-Structure and Function* **15**(2): 123-130.

Phillips N, Oren R, Zimmermann R, Wright SJ. 1999. Temporal patterns of water flux in trees and lianas in a Panamanian moist forest. *Trees-Structure and Function* **14**(3): 116-123.

Phillips N, Ryan M, Bond B, McDowell N, Hinckley T, Čermák J. 2003. Reliance on stored water increases with tree size in three species in the Pacific Northwest. *Tree Physiology* **23**(4): 237-245.

Phillips OL, Aragão LEOC, Lewis SL, Fisher JB, Lloyd J, López-González G, Malhi Y, Monteagudo A, Peacock J, Quesada CA, et al. 2009. Drought Sensitivity of the Amazon Rainforest. *science* **323**(5919): 1344-1347.

Pineda-García F, Paz H, Meinzer FC, Angeles G. 2015. Exploiting water versus tolerating drought: water-use strategies of trees in a secondary successional tropical dry forest. *Tree Physiology* **36**(2): 208-217.

Pineda-Garcia F, Paz H, Meinzer FC. 2012. Drought resistance in early and late secondary successional species from a tropical dry forest: the interplay between xylem resistance to embolism, sapwood water storage and leaf shedding. *Plant, Cell & Environment* **36**(2): 405-418.

Poorter L, McDonald I, Alarcón A, Fichtler E, Licona JC, Peña-Claros M, Sterck F, Villegas Z, Sass-Klaassen U. 2010. The importance of wood traits and hydraulic conductance for the performance and life history strategies of 42 rainforest tree species. *New Phytologist* **185**(2): 481-492.

Poorter L, van de Plassche M, Willems S, Boot RGA. 2004. Leaf Traits and Herbivory Rates of Tropical Tree Species Differing in Successional Status. *Plant Biology* **6**(06): 746-754.

Powell TL, Galbraith DR, Christoffersen BO, Harper A, Imbuzeiro H, Rowland L, Almeida S, Brando PM, Costa ACL, Costa MH. 2013. Confronting model predictions of carbon fluxes with measurements of Amazon forests subjected to experimental drought. *New Phytologist* **200**(2): 350-365.

Powell TL, Wheeler JK, de Oliveira AA, da Costa L, Carlos A, Saleska SR, Meir P, Moorcroft PR. 2017. Differences in xylem and leaf hydraulic traits explain differences in drought tolerance among mature Amazon rainforest trees. *Global Change Biology* **23**(10): 4280–4293.

R Core Team 2015. R: A Language and Environment for Statistical Computing (Version 3.3.2). Vienna, Austria: R Foundation for Statistical Computing.

Rowland L, Da Costa A, Galbraith D, Oliveira R, Binks O, Oliveira A, Pullen A, Doughty C, Metcalfe D, Vasconcelos S. 2015. Death from drought in tropical forests is triggered by hydraulics not carbon starvation. *Nature* **528**(7580): 119-122.

Sack L, Tyree MT, Holbrook NM. 2005. Leaf hydraulic architecture correlates with regeneration irradiance in tropical rainforest trees. *New Phytologist* **167**(2): 403-413.

Santiago L, Goldstein G, Meinzer F, Fisher J, Machado K, Woodruff D, Jones T. 2004. Leaf photosynthetic traits scale with hydraulic conductivity and wood density in Panamanian forest canopy trees. *Oecologia* **140**(4): 543-550.

Schönbeck L, Lohbeck M, Bongers F, Ramos M, Sterck F. 2015. How do Light and Water Acquisition Strategies Affect Species Selection during Secondary Succession in Moist Tropical Forests? *Forests* **6**(6): 2047.

Schwendenmann L, Pendall E, Sanchez-Bragado R, Kunert N, Hölscher D. 2015. Tree water uptake in a tropical plantation varying in tree diversity: interspecific differences, seasonal shifts and complementarity. *Ecohydrology* **8**(1): 1-12.

Sinacore K, Hall JS, Potvin C, Royo AA, Ducey MJ, Ashton MS. 2017. Unearthing the hidden world of roots: Root biomass and architecture differ among species within the same guild. *PLoS One* **12**(10): e0185934.

Stahl C, Burban B, Wagner F, Goret JY, Bompy F, Bonal D. 2013. Influence of seasonal variations in soil water availability on gas exchange of tropical canopy trees. *Biotropica* **45**(2): 155-164.

Turner BL, Engelbrecht BM. 2011. Soil organic phosphorus in lowland tropical rain forests. *Biogeochemistry* **103**(1-3): 297-315.

Tyree MT, Engelbrecht BM, Vargas G, Kursar TA. 2003. Desiccation tolerance of five tropical seedlings in Panama. Relationship to a field assessment of drought performance. *Plant Physiology* **132**(3): 1439-1447.

Tyree MT, Ewers FW. 1991. The hydraulic architecture of trees and other woody plants. *New Phytologist* **119**(3): 345-360.

Tyree MT, Sperry JS. 1989. Vulnerability of xylem to cavitation and embolism. *Annual Review of Plant Biology* **40**(1): 19-36.

Tyree MT, Velez V, Dalling J. 1998. Growth dynamics of root and shoot hydraulic conductance in seedlings of five neotropical tree species: scaling to show possible adaptation to differing light regimes. *Oecologia* **114**(3): 293-298.

Van Bavel C. 1966. Potential evaporation: the combination concept and its experimental verification. *Water resources research* **2**(3): 455-467.

van Breugel M, Hall JS, Craven D, Bailon M, Hernandez A, Abbene M, van Breugel P. 2013. Succession of ephemeral secondary forests and their limited role for the conservation of floristic diversity in a human-modified tropical landscape. *PLoS One* **8**(12): e82433.

von Ende CN 2001. Repeated-measures analysis: growth and other time-dependent measures. In: Scheiner SM, Gurevitch J eds. *Design and Analysis of Ecological Experiments*. New York: Oxford University Press, 134-157.

Wolfe BT, Sperry JS, Kursar TA. 2016. Does leaf shedding protect stems from cavitation during seasonal droughts? A test of the hydraulic fuse hypothesis. *New Phytologist* **212**(4): 1007-1018.

Wright SJ. 2010. The future of tropical forests. *Annals of the New York Academy of Sciences* **1195**(1): 1-27.

Wright SJ, Kitajima K, Kraft NJ, Reich PB, Wright IJ, Bunker DE, Condit R, Dalling JW, Davies SJ, Díaz S. 2010. Functional traits and the growth–mortality trade-off in tropical trees. *Ecology* **91**(12): 3664-3674.

Zhang Q, Manzoni S, Katul G, Porporato A, Yang D. 2014. The hysteretic evapotranspiration—Vapor pressure deficit relation. *Journal of Geophysical Research: Biogeosciences* **119**(2): 125-140.

Zimmermann B, Zimmermann A, Scheckenbach H, Schmid T, Hall J, van Breugel M. 2013. Changes in rainfall interception along a secondary forest succession gradient in lowland Panama. *Hydrology and Earth System Sciences* **17**(11): 4659-4670.

Tables

Table 1 Summary statistics and t-test results (Bonferroni-adjusted alpha for 9 tests: 0.0056) for average nocturnal sap velocities by seasons and forest age. All analyses based on trees for which data was collected in all seasons (N_{SF8} = 15, N_{SF25} = 25, N_{SF80} = 26). Data from July 29, 2015 to August 31, 2016.

Forest	Season	N	Nocturnal V_s [cm h^{-1}]	Standard Error	95% confidence interval	p-value
SF8	Wet 2015	15	0.86	0.52	1.12	0.12
	Dry 2016	15	0.51	0.56	1.20	0.37
	Wet 2016	15	-0.26	0.67	1.44	0.71
SF25	Wet 2015	25	-0.61	0.64	1.32	0.35
	Dry 2016	25	2.01	0.57	1.78	0.002*
	Wet 2016	25	-0.48	0.53	1.09	0.37
SF80	Wet 2015	26	0.18	0.44	0.91	0.69
	Dry 2016	26	1.90	0.39	0.79	<0.001*
	Wet 2016	26	0.16	0.35	0.72	0.65

* significant ($p < 0.05$)

Table 2 ANOVA table of generalized linear mixed model results of average sap velocities per season (M-1) and least square means pairwise comparison for average diel sap velocities between seasons by forest age (Tukey's single step). Analyses based on trees for which data was collected in all seasons (N_{SF8} = 15, N_{SF25} = 25, N_{SF80} = 26). Data from July 29, 2015 to August 31, 2016.

	Sum of Squares	Mean Square	Degrees of Freedom	F-value	p-value
Forest Age	26.26	13.13	2	1.28	0.28
Season	156.78	78.39	2	7.65	<0.001*
Forest Age : Season	45.36	11.34	4	1.11	0.36

Forest	Contrast	Estimate	Standard Error	t-value	p-value
SF8	Wet 2015 – Dry 2016	-0.54	1.17	-0.46	0.89
	Wet 2015 – Wet 2016	1.40	1.17	1.19	0.46
	Dry 2016 – Wet 2016	1.94	1.17	1.66	0.22
SF25	Wet 2015 – Dry 2016	-1.55	0.91	-1.72	0.20
	Wet 2015 – Wet 2016	-0.28	0.91	-0.31	0.95
	Dry 2016 – Wet 2016	1.28	0.91	1.41	0.34
SF80	Wet 2015 – Dry 2016	-3.02	0.89	-3.40	0.003*
	Wet 2015 – Wet 2016	0.13	0.89	0.15	0.99
	Dry 2016 – Wet 2016	3.15	0.89	3.55	0.002*

* significant ($p < 0.05$)

Table 3 Relative importance metrics and confidence intervals. Methods are AVRG (overall model contribution averaged over orderings of predictors) and LAST (model contribution given all other predictor already included in the model). Data include all trees (N_{SF8} = 19, N_{SF25} = 28, N_{SF80} = 27). Predictors are PPFD (photosynthetic photon flux density), VPD (vapor pressure deficit), Precip. (precipitation), VWC (soil volumetric water content), and WS (wind speed). Note that predictors are sorted by relative importance for each metric and forest combination. Overall model performance was 69, 66, and 86% for SF8, SF25, and SF80, respectively. A separate analysis of relative importance metrics on a subset of trees smaller than 15 cm DBH in SF25 and SF80 largely agrees with results from respective full models (Table S5).

				95% CI	
Forest	Method	Predictor	Rel. imp. [%]	upper	lower
SF8	AVRG	PPFD	47.96	42.36	52.7
	AVRG	VPD	28.88	24.83	32.97
	AVRG	Precip.	10.99	6.78	15.58
	AVRG	VWC	8.09	5.44	11.5
	AVRG	WS	4.08	2.22	7.08
	LAST	PPFD	40.32	23.23	58.74
	LAST	VWC	31.42	18.68	42.47
	LAST	Precip.	15.49	8.07	23.85
	LAST	VPD	9.86	3.87	18.62
	LAST	WS	2.92	0.24	7.67
SF25	AVRG	PPFD	39.54	34.64	44.32
	AVRG	VPD	31.00	26.76	34.88
	AVRG	Precip.	12.59	8.91	17.09
	AVRG	WS	9.86	6.25	13.94
	AVRG	VWC	7.01	5.43	8.68
	LAST	PPFD	34.35	16.63	53.57
	LAST	Precip.	21.35	12.15	31.94
	LAST	VPD	20.72	9.84	33.39
	LAST	WS	12.24	4.26	22.43
	LAST	VWC	11.35	5.11	18.4
SF80	AVRG	VPD	35.23	31.64	38.66
	AVRG	PPFD	27.73	24.51	30.89
	AVRG	VWC	17.73	14.9	20.56
	AVRG	WS	13.01	9.61	16.66
	AVRG	Precip.	6.29	4.35	8.54
	LAST	VPD	55.75	38.2	69.12
	LAST	PPFD	18.06	7.31	31.13
	LAST	WS	12.59	4.52	23.08
	LAST	Precip.	9.87	4.53	17.03
	LAST	VWC	3.72	0.37	10.57

761 **Figures**

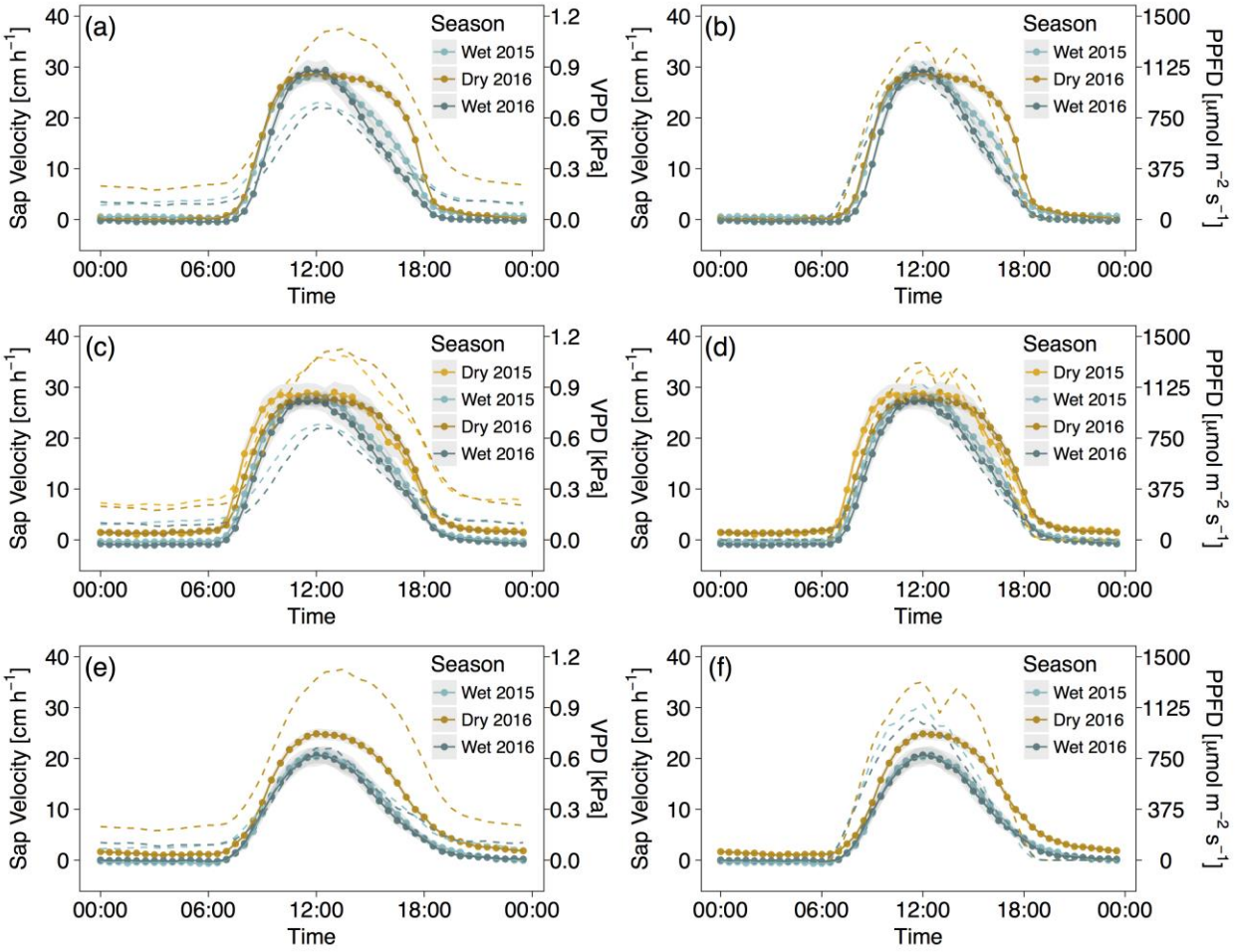

762

763 **Fig. 1** Diel patterns of sap velocities (cm h^{-1}) based on half-hourly averages from all trees in SF8 (a, b),
764 SF25 (c, d), and SF80 (e, f). Shaded areas represent 95% confidence intervals. The dashed lines indicate
765 half-hourly averages of vapor pressure deficit (VPD in kPa; a, c, e) and photosynthetic photon flux
766 density (PPFD in µmol m^{-2} s^{-1}; b, d, f).

767

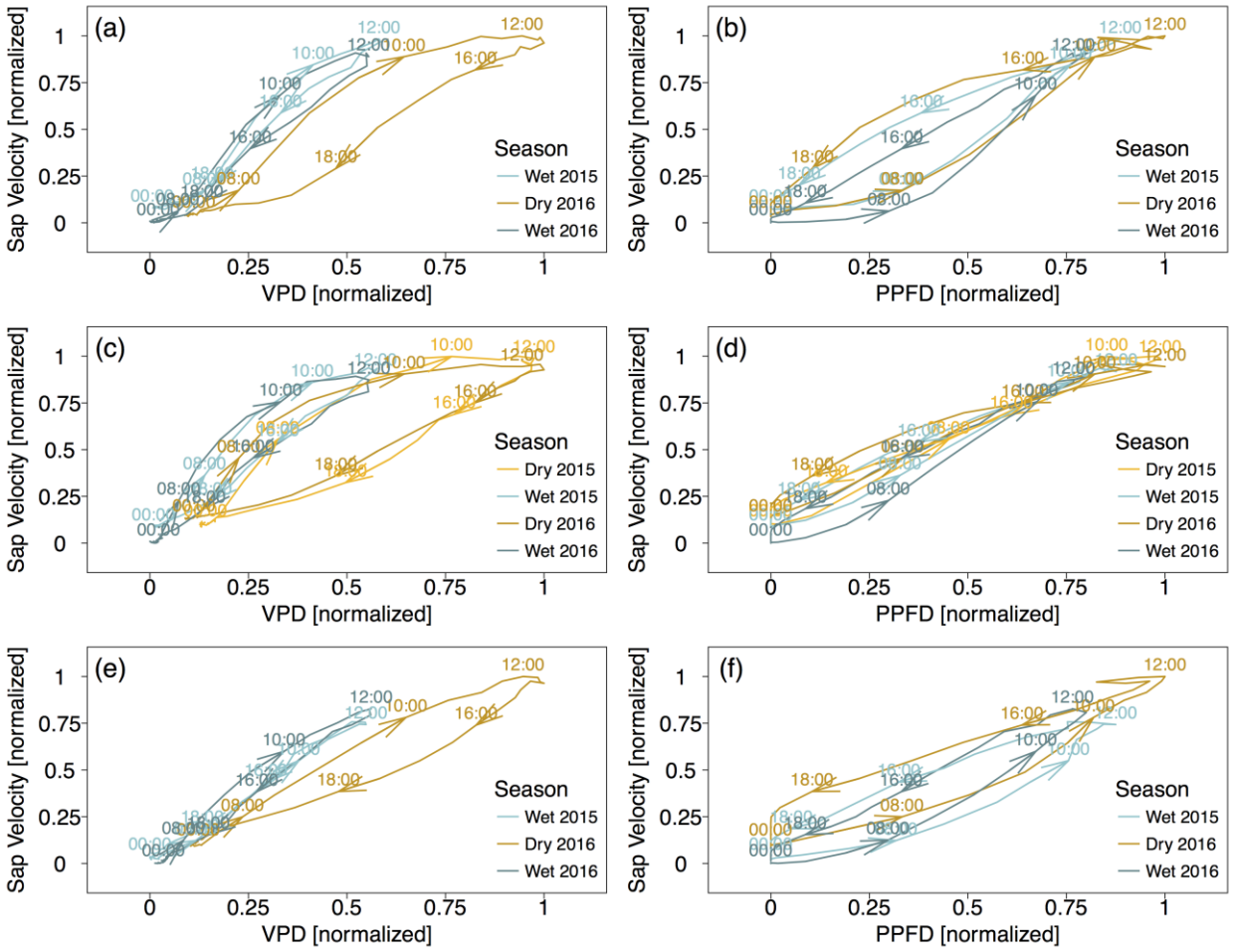

768

769 **Fig. 2** Hysteresis loops between normalized sap velocities and normalized vapor pressure deficit (VPD; a,
770 c, e) and normalized sap velocities and normalized photosynthetic photon flux density (PPFD; b, d, f) in
771 SF8 (a, b), SF25 (c, d), and SF80 (e, f). Arrows indicate direction of hysteresis.

772

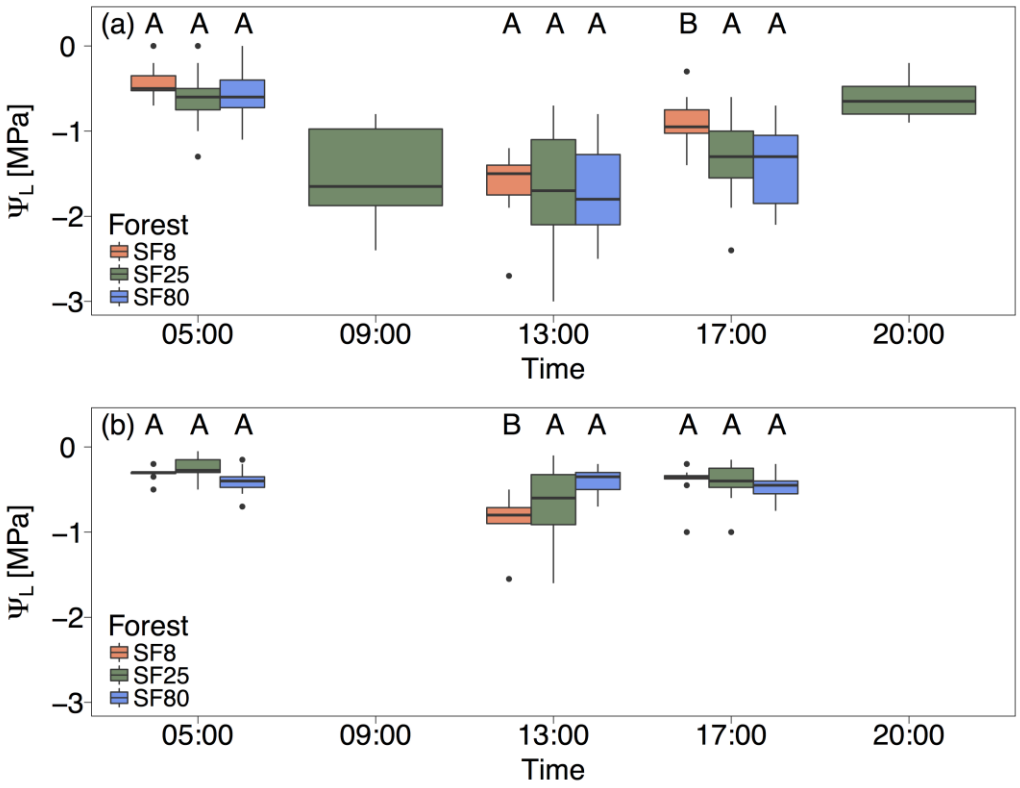

773

774 **Fig. 3** Leaf water potentials Ψ_L in MPa in the dry season (a; March 6-16, 2016) and wet season (b; July
775 26-28, 2016) for SF8 (orange), SF25 (green), and SF80 (blue). Horizontal lines inside boxes correspond
776 to the median, the lower and upper box boundaries correspond to first and third quartiles (25^{th} and 75^{th}
777 percentile, respectively), lower and upper whiskers extend no further than 1.5×IQR (inner quartile range)
778 from the first and third quartiles, and dots represent data points beyond this range. Letters indicate
779 significant differences in average leaf water potential between forests at a given sampling time as assess
780 via linear mixed model and least square means pairwise comparison. Data from 9:00 and 20:00 were only
781 collected in SF25 in the dry season.

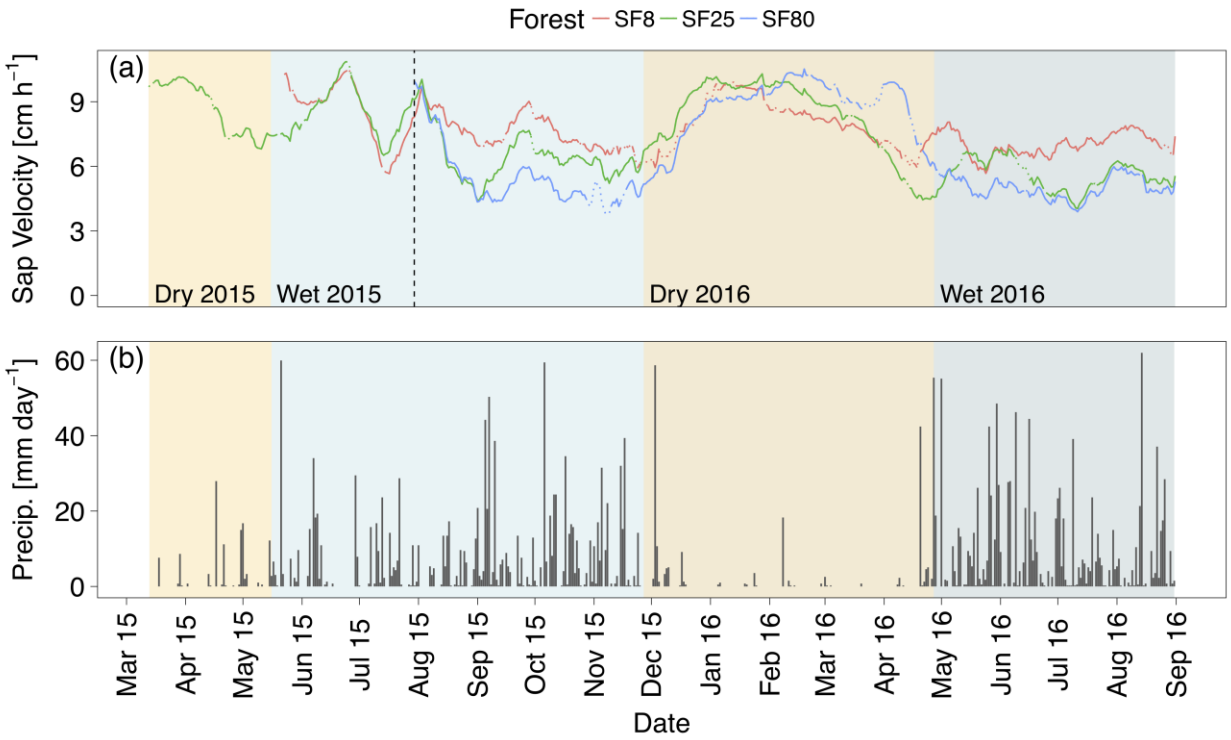

782

783 **Fig. 4** Time series of 3-week running mean sap velocities (cm h^{-1}; a) and precipitation (mm day^{-1}; b).
784 Shaded areas denote seasons (tan: dry, blue: wet). The dashed line indicates earliest date from which data
785 across all forest ages are available (July 29, 2015). Data from all trees are shown, with a minimum of 10
786 trees providing data per day out of 19, 28, and 27 trees in SF8, SF25, and SF80, respectively.

787

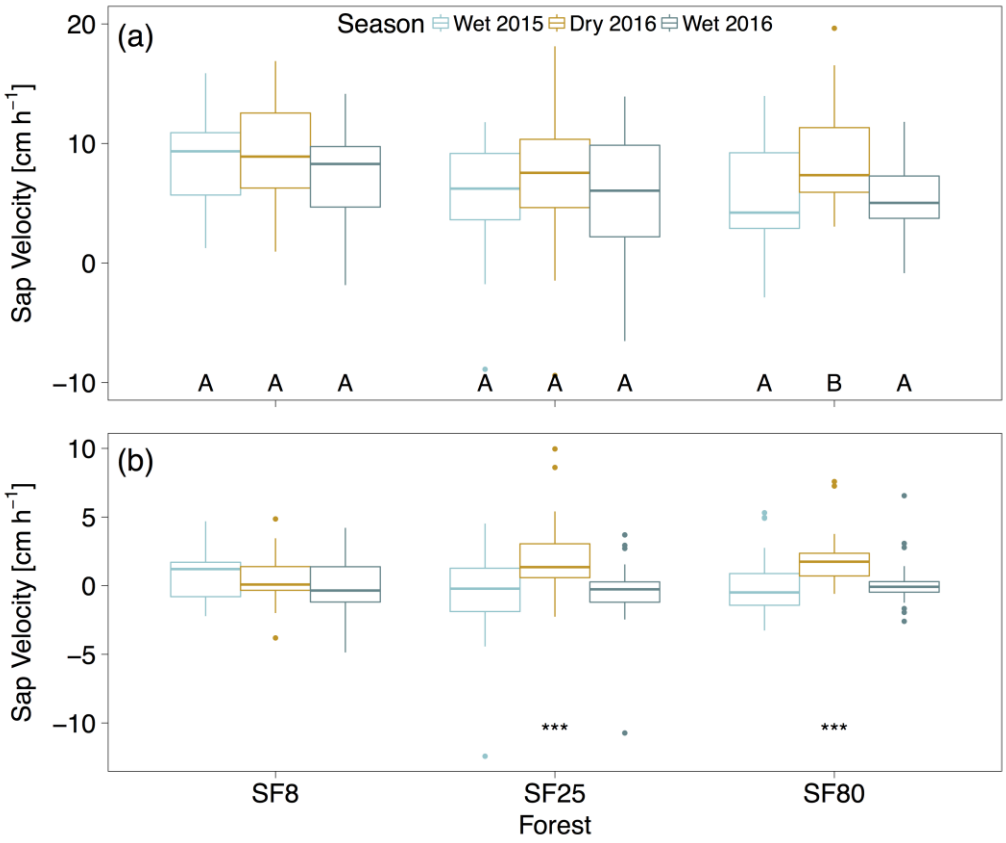

788

789 **Fig. 5** Linear mixed model results of diel (a) and nocturnal (b) sap velocities in cm h^{-1} based on trees for
790 which data was collected in all seasons (N_{SF8} = 15, N_{SF25} = 25, N_{SF80} = 26). Letters in A denote grouping,
791 with different letters indicating significant differences in sap velocities between seasons within a given
792 forest types ($\alpha < 0.05$; Tukey method). *** in B denotes nocturnal sap velocities that were significantly
793 different from 0. Data from July 29, 2015 to August 31, 2016. Horizontal lines inside boxes correspond to
794 the median, the lower and upper box boundaries correspond to first and third quartiles (25^{th} and 75^{th}
795 percentile, respectively), lower and upper whiskers extend no further than 1.5×IQR (inner quartile range)
796 from the first and third quartiles, and dots represent data points beyond this range.

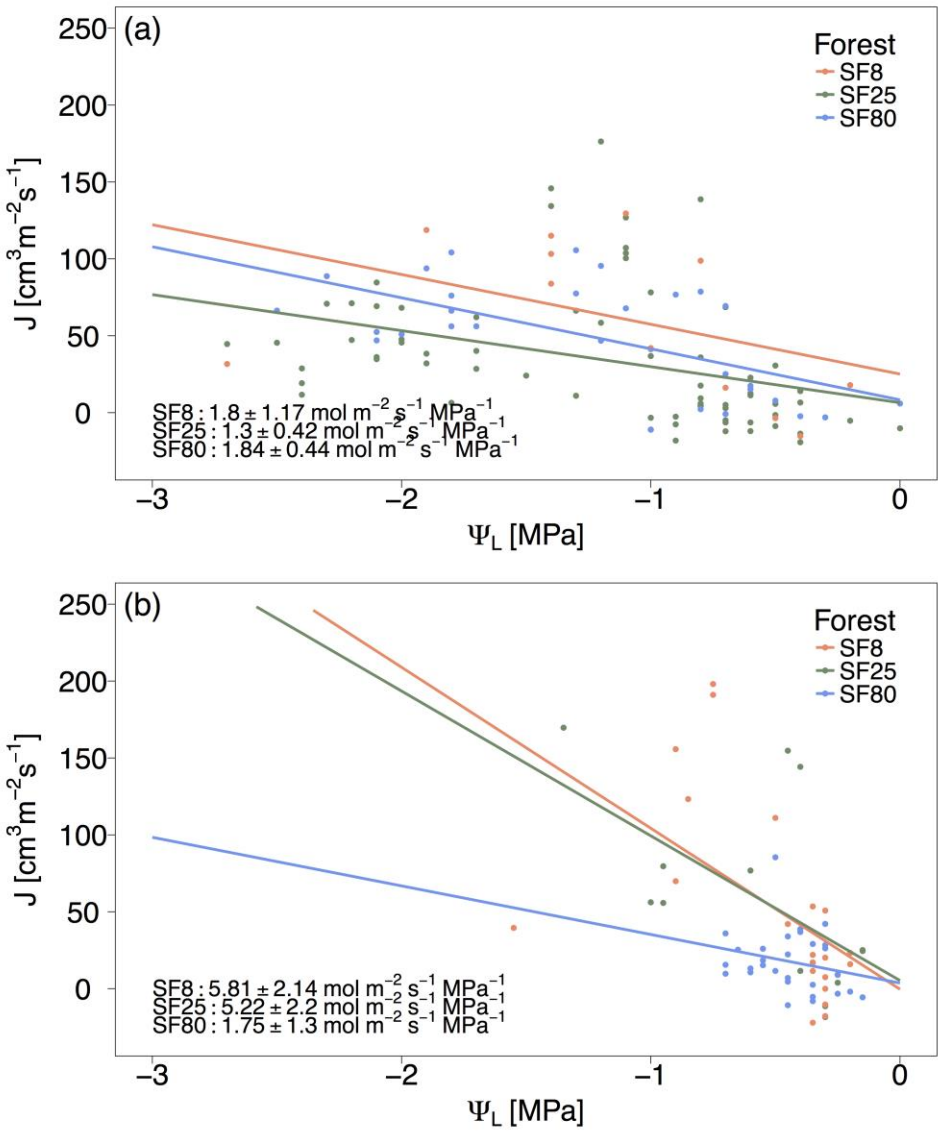

797

798 **Fig. 6** Leaf water potential Ψ_L (MPa) and corresponding sap flow J (cm^3 m^{-2} s^{-1}) in SF8 (orange), SF25
799 (green), and SF80 (blue) in the dry season (a) and wet season (b). J values were lagged up to 90 minutes,
800 based on highest correlation coefficient between (lagged) J and evaporative demand for a given tree on
801 the day of measurement. Darcy's law approximations and respective standard errors of sapwood-specific
802 conductivity K_s (mol m^{-2} s^{-1} MPa^{-1}) are given in the graphs.

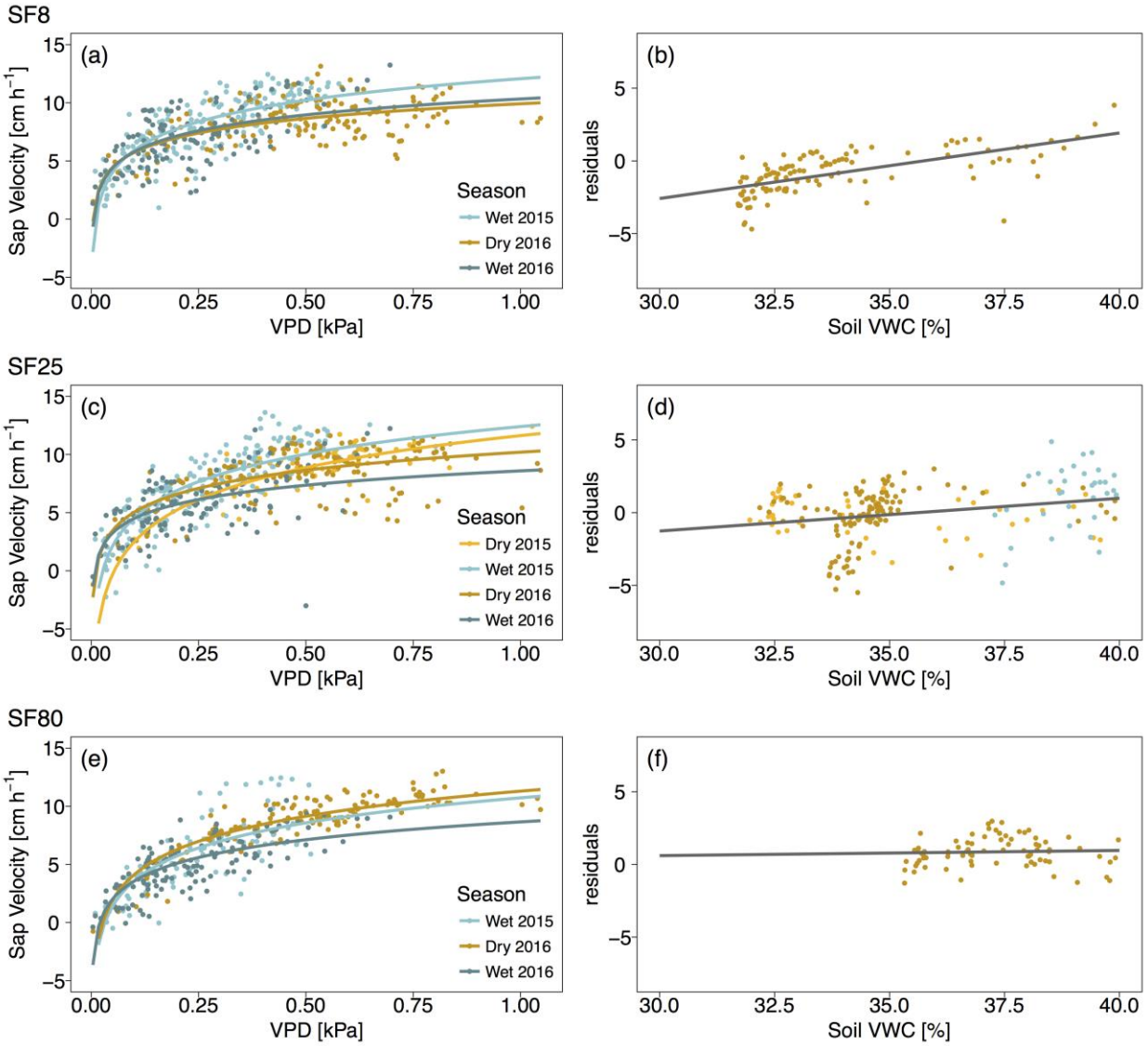

803

804 **Fig. 7** Linear regression of daily average VPD (kPa) and sap velocity V_s (cm h^{-1}; a, c, e), and residuals
805 plotted against volumetric water content (%) in the top 50 cm of the soil (b, d, f) in SF8 (a), SF25 (b), and
806 SF80 (c). VPD explained 48 % (SF8; a), 54 % (SF25; c), and 71 % (SF80; e) of variance in V_s. Linear
807 regression between residuals and soil VWC was significant in SF8 (b; $R^2 = 0.42$, $p < 0.001$) and SF25 (d;
808 $R^2 = 0.7$, $p < 0.001$), and was non-significant in SF80 (f). Note how soil VWC does not go below 40% in
809 the wet season in either SF8 (b) or SF80 (f). Single-variable regression of PPFD and V_s explained 60%,
810 59%, and 66% in SF8, SF25, and SF80, respectively, with similar relationships between residuals and
811 VWC as above (Figure S2).

812

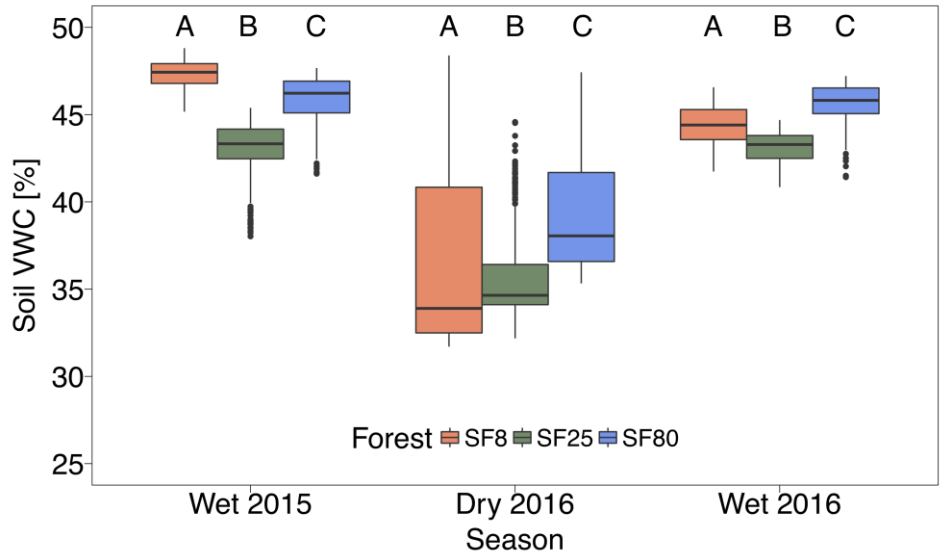

Fig. 8 Soil volumetric water content (%) in the top 50 cm of the soil in SF8 (orange), SF25 (green), and SF80 (blue). Data from July 29, 2015 to August 31, 2016. Horizontal lines inside boxes correspond to the median, the lower and upper box boundaries correspond to first and third quartiles (25^{th} and 75^{th} percentile, respectively), lower and upper whiskers extend no further than 1.5×IQR (inner quartile range) from the first and third quartiles, and dots represent data points beyond this range. Letters indicate significant differences in VWC between forests per season as assess via linear mixed model and least square means pairwise comparison.

Supporting Information

Fig. S1 Boxplots of leaf water potentials at different canopy positions from eight species (N=36) in SF80.

Fig. S2 Minimum number of working sap flow sensors and resulting standard deviation of average sap velocity data for all forests.

Fig. S3 Linear regression of daily average PPFD (μmol m^{-2} s^{-1}) and sap velocity V_s (cm h^{-1}), and model residuals plotted against volumetric water content (%) in the top 50 cm of the soil.

Fig. S4 Time series of 3-week running mean sap velocities and sum of daily precipitation, excluding four *Annona spraguei* and one *Casearea arborea* in SF25 due to their long-term dormancy at the end of the dry season 2016.

Fig. S5 Boxplot of average daily Omega decoupling coefficients for all forests and seasons.

Table S1 Overview of sap flow site characteristics, including GPS coordinates, slope, aspect, slope length, and elevation.

Table S2 Overview of instrumented species and their phenology, relative canopy position, diameter at breast height (cm), and wood density (g cm^{-3}).

Table S3 Overview of instrumented species, respective sampling periods, and number of days where no data was collected (e.g. due to equipment failure).

Table S4 ANOVA table of generalized linear mixed model results (M-2) and parameter estimates and p-values based on Markov Chain Monte Carlo method with 1000 iterations.

Table S5 Relative importance metrics and confidence intervals of trees < 15 cm DBH trees (NSF8 = 19, NSF25 = 11, NSF80 = 13).

Table S6 Relative importance metrics and confidence intervals for SF25, excluding four *Annona spraguei* and one *Casearia arborea* due to their long-term dormancy at the end of the dry season.